**PASJ:** Publ. Astron. Soc. Japan **45**, 661–668 (1993)

# Diffuse Emission from the Coma–A1367 Supercluster and Cosmic X-Ray Background

Yuzuru TAWARA and Mitsunobu KAWADA
*Department of Astrophysics, School of Science, Nagoya University, Chikusa-ku, Nagoya 464-01*
and
Katsuji KOYAMA
*Department of Physics, Faculty of Science, Kyoto University, Sakyo-ku, Kyoto 606-01*

(Received 1993 March 19; accepted 1993 May 21)

**Abstract**

We carried out scanning observations with the Ginga satellite of the near-by Coma–A1367 supercluster and the void regions. We discovered 4 new sources within these regions with a detection limit of $5 \times 10^{-12}$ erg s$^{-1}$ cm$^{-2}$ (2–10 keV). This rate corresponds to about $10^2$ sources sr$^{-1}$, and lies on the extrapolated $\log N - \log S$ line determined by Piccinotti et al. (1982, AAA 142.012). We also compiled blank-sky data in order to determine the surface brightness of the cosmic X-ray background (CXB), mostly taken as background observations of extragalactic sources. By comparing diffuse emission from these two data sets, we found no significant difference between their mean fluxes and distributions. No significant correlation between the surface brightness and the galaxy number density for the region was found, except for the clusters, themselves. We also compared the X-ray flux between the supercluster and void regions, and set a $3\sigma$ upper-limit for the excess emission of the supercluster region to be $9.5 \times 10^{-13}$ erg cm$^{-2}$ s$^{-1}$ (arcdeg)$^{-2}$.

**Key words:** A1367 — Coma cluster —Cosmic X-ray background — Supercluster — Void

## 1. Introduction

A supercluster is the largest structure in the universe known at present. It comprises many clusters making up a chain-like or sheet-like structure. The Coma–A1367 supercluster is one of the nearest and, hence, most extensively studied superclusters.

The X-ray emission from superclusters has been investigated by several authors. Murray et al. (1978) pointed out that three Uhuru sources positionally coincide with 3 superclusters of the Abell catalog. The probability for a chance coincidence is lower than 0.3%. They estimated that the X-ray flux from an individual cluster is insufficient to explain the observed flux, and therefore concluded that the inter-cluster medium is responsible for the X-ray emission. The inferred flux is $3 \times 10^{45}$ erg s$^{-1}$ (2–10 keV band) and the total mass of the inter-cluster hot gas is 10 times larger than the sum of the masses of the individual galaxies. However, Pravdo et al. (1979), using the HEAO–A1 data, claimed that no excess emission was observed from the superclusters. Using the more complete data base of the HEAO–A2 experiments, Persic et al. (1988) compared the mean surface brightness of ten superclusters in the catalog of Bahcall and Soneira (1984) to that of the blank sky, finding no significant difference between the two values. They thus concluded that the supercluster X-ray emission is less than $2 \times 10^{-12}$ erg s$^{-1}$ cm$^{-2}$ (arcdeg)$^{-2}$ at the $3\sigma$ level. They also searched for smaller angular-size superclusters and set an upper-limit for the X-ray surface brightness of $1 \times 10^{-12}$ erg s$^{-1}$ cm$^{-2}$ at the $3\sigma$ level.

Jahoda and Mushotzky (1989), using the same HEAO–A1 data base, estimated an excess emission from the direction of the Great Attractor and found an excess flux of $(7.8 \pm 1.0) \times 10^{-13}$ erg s$^{-1}$ cm$^{-2}$ (arcdeg)$^{-2}$. If this was due to inter-cluster hot gas, the mass would be about 25% of the total mass of the "Great Attractor." However, since the "Great Attractor" is behind the galactic plane, a careful estimate of the galactic disk components was required. Using the Ginga satellite, Day et al. (1991) have carried out scanning observation over the Shapley supercluster, and set a $3\sigma$ upper-limit of excess emission to be $2.0 \times 10^{-13}$ erg s$^{-1}$ cm$^{-2}$ (arcdeg)$^{-2}$.

Thus, at present there is no convincing evidence for any inter-cluster hot gas. In order to detect or to set a more severe upper limit for X-ray emission from the supercluster medium, we carried out scanning observations over the Coma–A1367 regions.

## 2. Observations

### 2.1. *Scans of Coma–A1367 Region*

The first scanning observations were made on 1988 December 22–25, with 4 scan paths (designated as paths A,

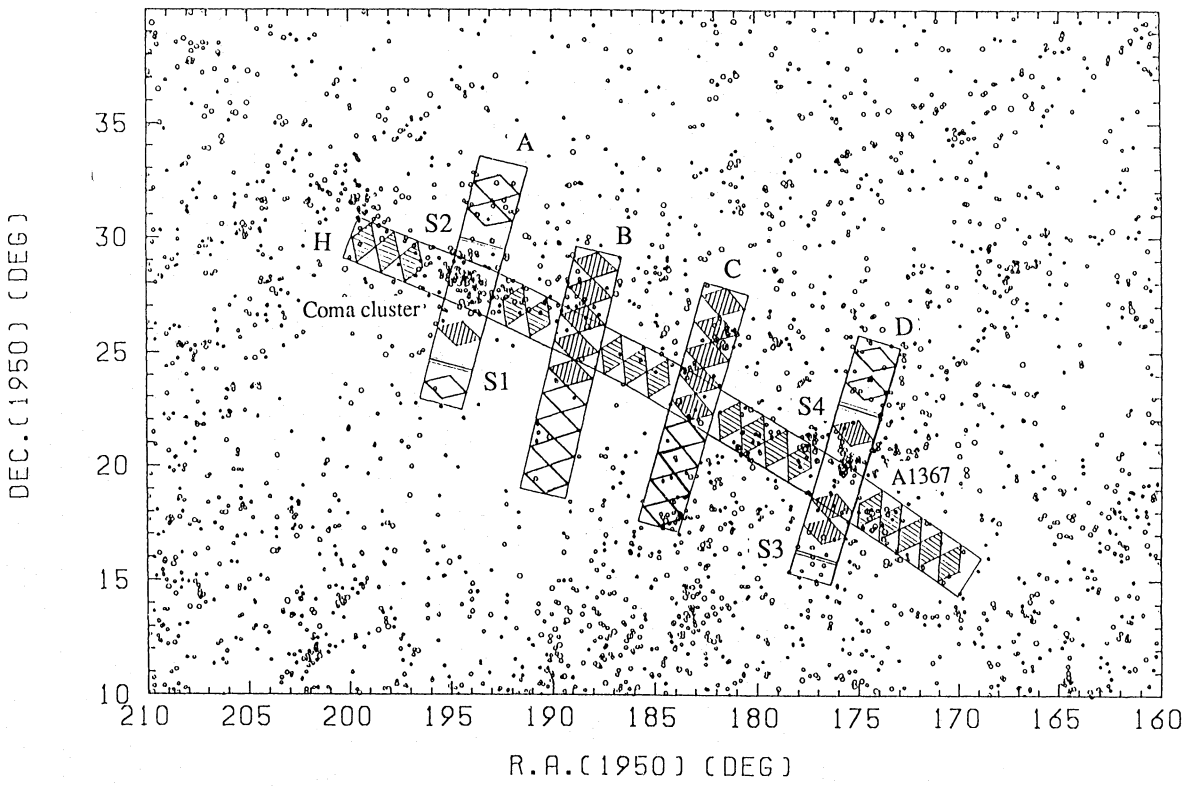


Fig. 1. Scan region overlaid on the optical galaxy map. The solid squares are the scan paths with FWHM of the LAC field of view. The positions of new point sources are indicated by thick bars with errors (thin bars). The diamonds are the positions used to examine the diffuse X-rays, the hatched diamonds as supercluster region including 2 clusters and 5 groups of galaxies and open diamonds as Void.

B, C, and D), roughly perpendicular to the line connecting the Coma and A1367 clusters. Parallel scans (path H) were then made on 1989 May 18–20. These scans are shown in figure 1 overlaid on an optical map of the galaxies. The observation data was selected according to the minimum background phase of the 37 d periodic variations (for background variation, see Hayashida et al. 1989).

The LAC field of view is 1° and 2° (FWHM) along and perpendicular to the scanning path, respectively. The scanning speed was typically 0.°5 $\mathrm{min}^{-1}$. Each scanning profile comprised several sequential multi-scans in order to obtain better photon statistics.

The data accumulation was made in the MPC–1 mode, in which 48 energy channels from the top and the mid layers were recorded separately for each counter (for details see Turner et al. 1989).

While the energy channels from 0 to 31 are roughly proportional to the X-ray energy with a coefficient of 0.56 keV $\mathrm{channel}^{-1}$, the energy width is doubled above the 32-nd channel. The highest energy (at the 48-th channel) is 38 keV. For X-ray signals, we usually exclude the data above the 32-nd channel (above 18 keV), since most of the signals are due to the particle background. Below the 15-th channel (less than about 9.2 keV), most of the X-rays fall within the top layer. Thus, in order to utilize the best S/N ratio, we used the top layer data.

### 2.2. *Cosmic Diffuse X-Rays*

Since Ginga did not have an imaging instrument, the nominal mode for observing weak point sources was a comparison of the source with the nearest blank sky. Between 1987 April and 1989 August, we selected 51 blank-sky background observations with a galactic latitude of above 40°. These positions are plotted in figure 2 along with the galactic coordinates. In this paper these diffuse X-rays are referred to as the Cosmic X-Ray Background (CXB).

### 2.3. *Subtraction of Particle Background*

Since we are interested in the diffuse X-rays, we need to subtract the particle background from the scanning

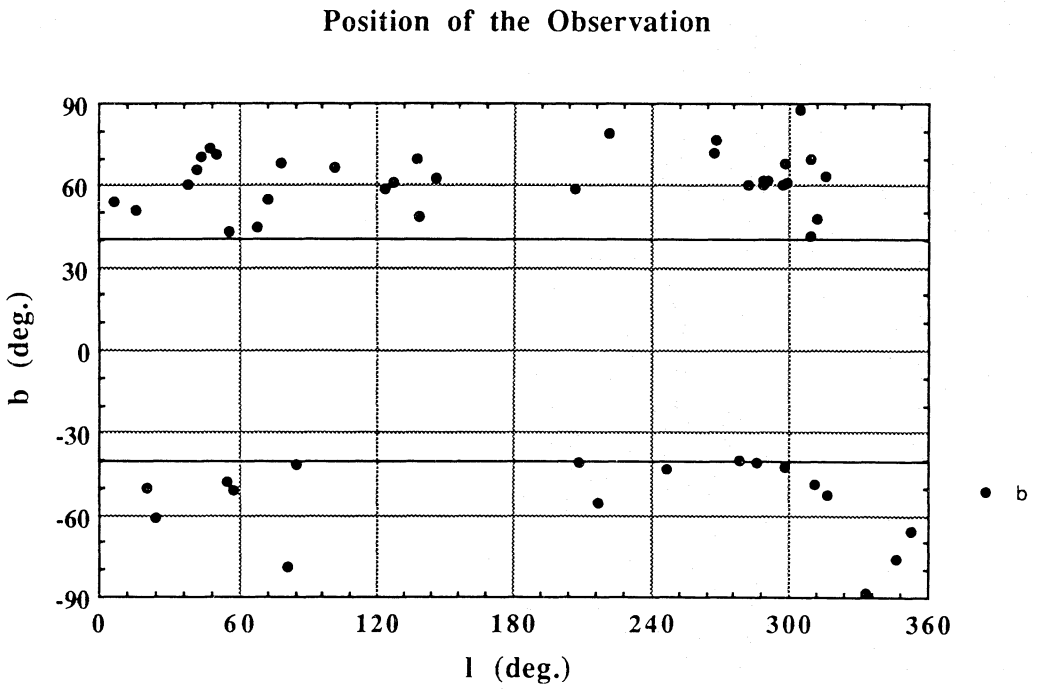


Fig. 2. Position of the data points for the CXB (see subsection 2.2).

and pointing data. We applied the method developed by Awaki et al. (1991), which we briefly review here. We assumed that the particle background is the flux when the dark earth is occulting the LAC field of view. This assumption was proven to be correct, and is demonstrated later. We therefore selected the dark Earth data observed during the period from 1987 April to 1990 February.

In order to optimize the reliability of the background estimation, we set rather severe constraints for the data selection: 1) The geomagnetic cutoff rigidity is greater than 9 GeV $c^{-1}$, 2) There is no contamination from geomagnetically trapped particles, 3) There is no contamination from solar X-rays.

Since the particle background is a function of the satellite position, we classify the fifteen satellite orbits as being eight "high-background orbits" which pass through the South Atlantic Anomaly (SAA), and the other seven as being "low-background orbits." After passage through the SAA, the background caused by radioactivity with short half lives (6 min and 41 min) is dominant. We therefore divided the "high-background orbits" into two parts: one "before the SAA passage" and the other "after the SAA passage." We thus composed three subsets corresponding to the low-background orbits and the high-background orbits before and after the SAA passage.

The total accumulation times for the particle background were $3.6 \times 10^5$ s, $1.1 \times 10^5$ s, and $1.0 \times 10^5$ s for the low-background orbits and the high-background orbits before and after SAA passage, respectively. We found that the particle background for each subgroup is given as a function of the $SUD$ rate (the LAC count rate above 38 keV):

$$\text{Particle background (count s}^{-1}\text{ ch}^{-1}) = A + B \times SUD \text{ (counts s}^{-1}), \quad (1)$$

where coefficients $A$ and $B$ for each energy channel of each layer were determined separately for the three subsets: the low- and high-background orbits before and after the SAA passage. The reproducibility of particle background using this method is better than 0.3 count $s^{-1}$. This level is nearly the same as that of Hayashida et al. (1989), in which a more complicated multi-parameter formula was developed. The advantage of the present method is that we could estimate the absolute flux of diffuse X-rays.

## 3. Results

### *3.1. Point Sources from the Coma–A1367 Region*

The scan profiles in the 1.1–9.2 keV energy range (1–15 ch) of the top layer after subtracting the particle background are given in figure 3. In addition to the strong X-ray emission from the Coma and A1367 clusters, several point-like sources are noticeable in the scan profiles along paths A and D.

In order to pick up these resolved point sources, we fitted the overall scan profile along each path to a lin-

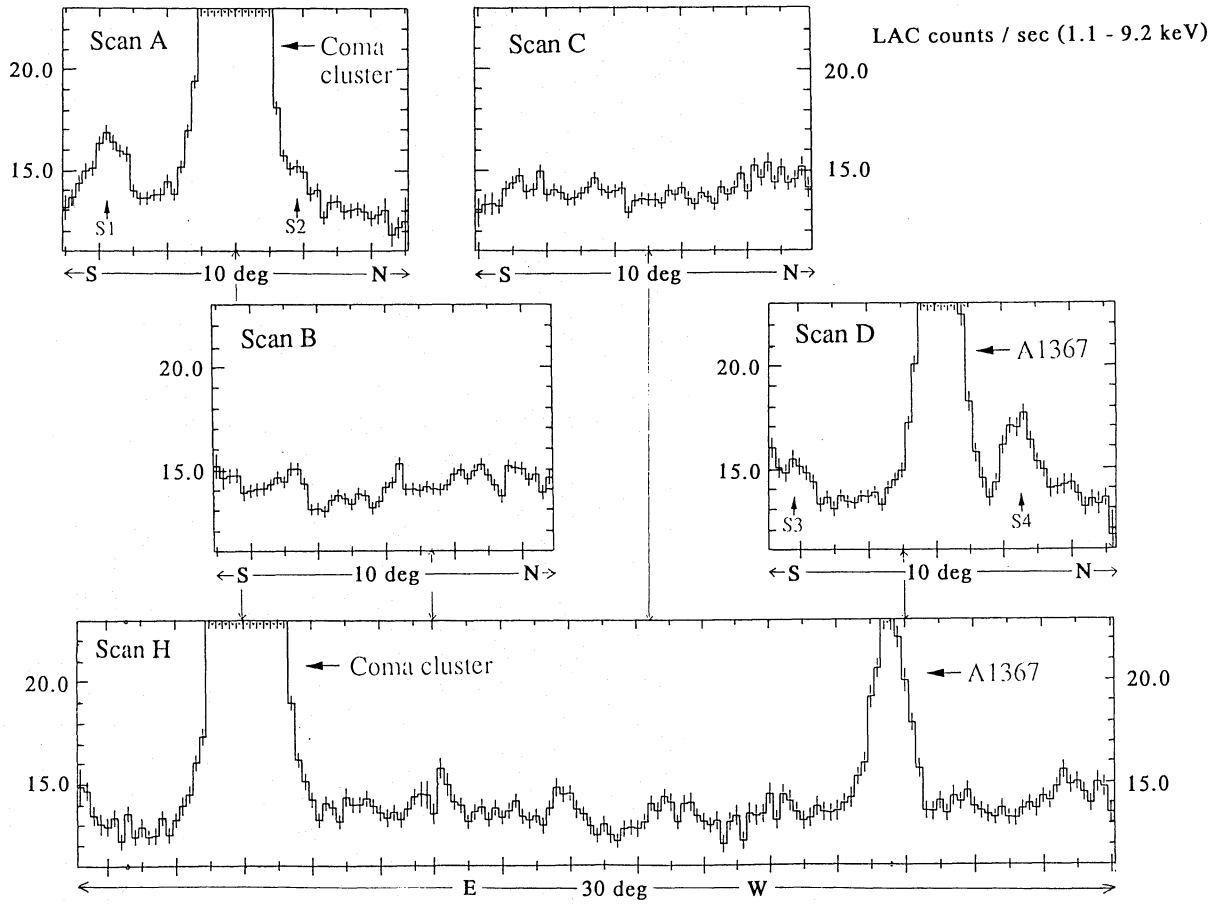


Fig. 3. Scanning profiles in the 1.1–9.2 keV bands from the Coma–A1367 region.

Table 1. New sources detected in a scan observation of the Coma–1367 region.

| # | R.A.* | Dec.* | Intensity (c s $^{-1}$)** |
|---|---|---|---|
| S1 ..... | 194.°91 | 24.°50 | $2.8 \pm 0.4$ |
| S2 ..... | 193.°47 | 29.°82 | $2.1 \pm 0.3$ |
| S3 ..... | 177.°03 | 16.°01 | $2.0 \pm 0.4$ |
| S4 ..... | 174.°89 | 22.°43 | $4.4 \pm 0.2$ |

* Center of error box. Size of error box is $0.°2 \times 4°$ for this 1-dimensional scan.

** LAC c s$^{-1}$: 2–10 keV, 1 c s$^{-1}$=0.1 mCrab.

ear background plus a point-source model (Forman et al. 1978). At first, a linear background with no point source model was tried, varying the intensity and slope of the linear background so as to minimize $\chi^2$. We then added one point source and re-tried the $\chi^2$ fit with two additional free parameters: the intensity and linear position of the source. This sequence was repeated by adding the point sources one by one. The statistical significance for the existence of the sources was tested by determining the decrease in $\chi^2$ when a new source was added to the model. If the decrease in $\chi^2$ was less than 30, the fitting procedure was then terminated. The probability, by chance, to decrease 30 in $\chi^2$ with 2 degrees of freedom (intensity and linear position of one point source) was $3 \times 10^{-7}$. This probability was almost the same as that for exceeding $5\sigma$ in a Gaussian distribution ($6 \times 10^{-7}$). Therefore, the threshold for the detection of a point source was regarded as being roughly $5\sigma$.

Using this procedure we picked up 4 new sources at the positions given in the scan path (figure 1): the results are summarized in table 1. Because of the relatively wide error boxes of $0.°2 \times 1.°0$ for these sources, there are several possible candidates in the radio, infrared, and optical bands. And detailed analysis of the identification will be described in a separate paper to be called "Ginga slew survey."

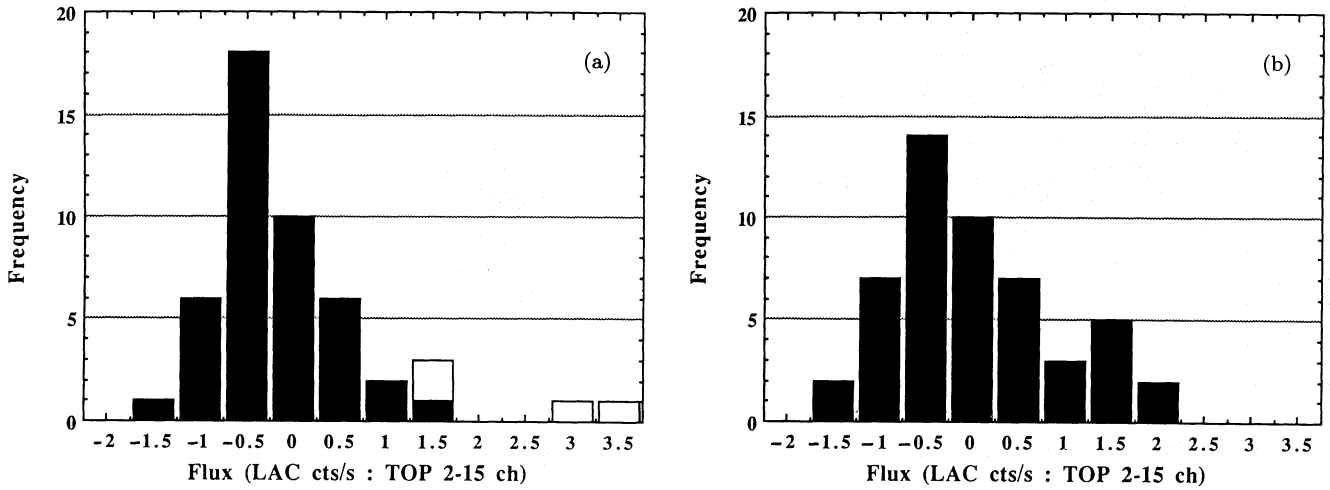


Fig. 4. Distribution of the diffuse flux with the top layer from the Coma–A1367 region (a) and that of CXB (b), where the fluxes are defined as the excess above a mean values of 14.05 count $s^{-1}$ (a) and 14.11 count $s^{-1}$ (b), respectively. The open squares indicate that the flux includes that from the new point sources.

### *3.2. Diffuse X-Ray from Coma–A1367 Region and CXB*

We accumulated the data for the diffuse X-rays as follows: since the extent of detector response along the scan path is 1° (FWHM), we divided each scan profile into 1° intervals. For the crossing points of two scans, we selected data with better statistics. The ±1° region from each point source was regarded as being one data point. The flux was set as that of a point-source. We excluded the regions where the contributions of Coma and A1367 were found to be significant, and ended with a total of 48 data points. They are indicated by diamonds and thick bars (the data for new point sources) in figure 1. These excluded regions have sizes of $(4 \times 9)h_{50}^{-1}$ Mpc for the Coma cluster and $(4 \times 6)h_{50}^{-1}$ Mpc for the A1367 cluster, respectively, along with each scan direction, where $h_{50}$ is the Hubble constant normalized by 50 km $s^{-1}$ $Mpc^{-1}$. The distribution of the excess flux above the mean is given in figure 4a, where the mean flux with the top layer is 14.05 counts $s^{-1}$.

We accumulated another data set for the CXB. In this case, the observations were pointing at 51 blank sky regions (figure 2). The mean flux in the 2–15 energy channels of the top layer was 14.11 counts $s^{-1}$, with a standard deviation of 0.97 counts $s^{-1}$. The distribution of the CXB is given in figure 4b, where the fluxes are defined as the excess above the mean value.

## 4. Analysis and Discussion

### *4.1. Mean Flux of Coma–A1367 Region and CXB*

The mean flux levels of Coma–A1367 and CXB are 14.05 and 14.11 counts $s^{-1}$, respectively. The flux of CXB corresponds to $6.5 \times 10^{-8}$ erg $s^{-1}$ $cm^{-2}$ $sr^{-1}$, which is in excellent agreement with that of Marshall et al. (1980) of $6.2 \times 10^{-8}$ erg $s^{-1}$ $cm^{-2}$ $sr^{-1}$, taking into account possible systematic errors of the two different instruments. We are thus convinced that the subtraction of the particle background was properly made, using the method of Awaki et al. (1991), in which the particle background was represented by the dark Earth data.

Since the total accumulation time for these data sets is large, the statistical error for one data point is estimated to be less than 0.01 count $s^{-1}$. The $1\sigma$ error for the source confusion noise is about 0.7 count $s^{-1}$ for the LAC field of view (Hayashida et al. 1989; also see next section). Since we have about 50 fields for each data sets, this source confusion error is reduced to 0.1 count $s^{-1}$. Thus, a significant error is attributable to the systematic error of the particle background subtraction. With our method, this error is estimated to be 0.3 count $s^{-1}$ (Awaki et al. 1991). Since this systematic error does not obey Poisson statistics, we cannot estimate the accurate error for the mean flux of these two data sets; however, the observed difference of 0.06 count $s^{-1}$ is significantly smaller than any systematic error of 0.1 count $s^{-1}$ (source confusion noise) or 0.3 count $s^{-1}$ (uncertainty of the particle background). We thus conclude that there is no significant difference between the mean flux of the Coma–A1367 region and CXB.

### *4.2. Fluctuation of the Diffuse Flux*

We have examined whether the flux distribution of the Coma–A1367 regions is different from that expected from the $\log N - \log S$ relation determined by Piccinotti et al.

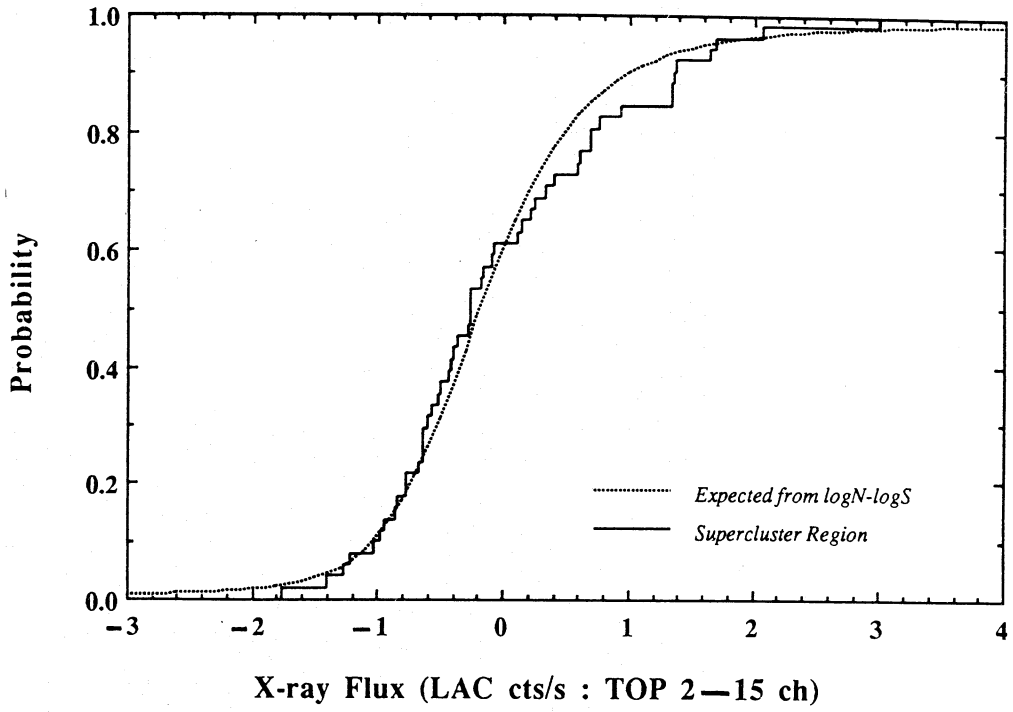


Fig. 5. Probability function of the simulated flux (dotted lines) and observed flux from the Coma–A1367 region (solid line).

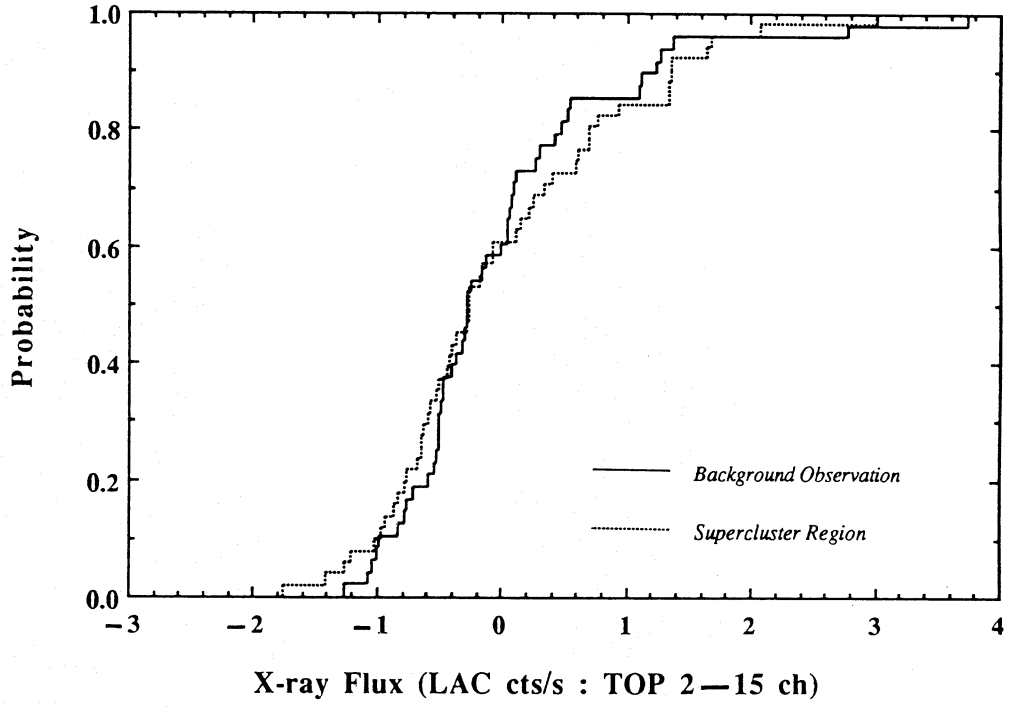


Fig. 6. Probability function of the observed flux from CXB (solid line) and that of the Coma–A1367 region (dotted line).

Table 2. Difference of the surface brightness between the supercluster and the void.

| Data Set | DS1 | DS2 |
|---|---|---|
| scan | A,B,C,D | A,B,C,D,H |
| mean flux (LAC c $s^{-1}$) Region I | $14.09 \pm 0.18$ | $13.83 \pm 0.32$ |
| mean flux (LAC c $s^{-1}$) Region II | $13.76 \pm 0.18$ | $13.76 \pm 0.35$ |
| flux difference (RegionI–II) | $0.33 \pm 0.25$ | $0.07 \pm 0.47$ |
| $3\sigma$ upper limit (erg $cm^{-2}$ $s^{-1}$ $beam^{-1}$: 2–10 keV) | $1.9 \times 10^{-12}$ | $3.5 \times 10^{-12}$ |

(1982). Here, we assumed that the $\log N - \log S$ relation can be extended to fainter sources which can be detected with Ginga's sensitivity, as already proved by Hayashida (1990) and Kondo (1991). For this purpose, we calculated the expected LAC flux in the 2–15 channels of the top layer using the method of Condon (1974). We then examined this model data set as well as the observed data set of the Coma–A1367 region, using the Kolmogorov–Smirnov test. The probability distribution for these two data sets is given in figure 5. The maximum difference between these two curves is 0.09 from 48 data points. If we set the 90% confidence level, the allowed maximum value for the difference of two curves is 0.17. We thus found no significant difference between the simulated CXB data and the observed data near to the Coma–A1367 region.

We also tested a more direct comparison between the observed data sets of CXB and the Coma–A1367 regions in figure 6. In this case the maximum difference was 0.1; we again found no significant differences between these two samples.

### *4.3. Supercluster and Void Region*

Since the present scanning observations cover both the supercluster and part of the void region, we tried to examine whether or not there is any significant difference between the surface brightness of the supercluster and the void. We tentatively divided these scan regions into the two groups given in figure 1. Region I (indicated by hatched diamonds) is regarded as being a supercluster region which includes 2 clusters and 5 groups of galaxies (Gregory and Thompson 1978); the remaining part is region II (indicated by open diamonds) and is the void. As previously noted, the largest flux error is due to the particle background subtraction. This systematic error becomes larger when the daily observation period becomes longer. We thus examined two kinds of data sets: (DS1), the scan A–D obtained during 3 d, which is expected to have a smaller particle background but larger Poisson fluctuations due to a small number of independent data, and (DS2), the scan A–D+scan H, obtained in two observational periods separated by 6 months, which are expected to have a larger particle background, but smaller Poisson fluctuations. For both data sets, we excluded the data points of the new 4 sources as well as the Coma and A1367 clusters

For these 2 data sets (DS1 and DS2) we found that for the mean flux from regions I and II, the upper limit on the difference between these regions, is obtained as shown in table 2. Here, the quoted $1\sigma$ errors include the statistical error, the source confusion noise, and the error of reproducibility for particle background noise. For DS1, the confusion noise is dominant, whereas that for DS2 is the particle background error. The flux differences between the two regions are both within the $3\sigma$ upper-limit. For a more accurate DS1, the $3\sigma$ upper-limit for the excess emission of supercluster in the 2–10 keV band is $9.5 \times 10^{-13}$ erg $cm^{-2}$ $s^{-1}$ $(arcdeg)^{-2}$, which is 5% of the CXB, and is nearly the same as the upper limit for the optically selected supercluster, with an angular size of less than 2° (Persic et al. 1990; Day et al. 1991).

Assuming the angular size of the Coma–A1367 supercluster to be about 35° long and 5°–10° wide, and its solid angle to be about $260(arcdeg)^2$, the total X-ray flux of the supercluster is estimated to be less than $2.5 \times 10^{-10}$ erg $s^{-1}$ $cm^{-2}$, or about $5 \times 10^{44} h_{50}^{-2}$ erg $s^{-1}$. If we further assume that the depth of the supercluster is equal to its width, the total volume is then about $1.4 \times 10^4 h_{50}^{-3}$ $Mpc^3$. The plasma density of the inter cluster gas with a temperature $kT$ is thus lower than $1.0 \times 10^{-5} (kT/10\ keV)^{-1/4} h_{50}^{3/2}$ $cm^{-3}$, and the total gas mass is less than $4 \times 10^{15} (kT/10\ keV)^{-1/4} h_{50}^{-3/2} M_\odot$.

## 5. Summary

(1) We discovered 4 new sources with a detection limit of $5 \times 10^{-12}$ erg $s^{-1}$ $cm^{-2}$ (2–10 keV). This rate is about $10^2$ sources $sr^{-1}$, and lies on the extrapolated $\log N - \log S$ line determined by Piccinoctti et al. (1982).

(2) We found no significant difference in the mean flux and on its distribution between the Coma–A1367 region and the CXB.

(3) We set a $3\sigma$ upper-limit on the excess emission of the Coma–A1367 supercluster to be $9.5 \times 10^{-13}$ erg $cm^{-2}$ $s^{-1}$ $(arcdeg)^{-2}$.

The authors thank Dr. Awaki for his contribution in the early stage of this work. The data analysis was carried out using the M380 computer of the High Energy Laboratory of Nagoya University.

## References

Awaki, H., Koyama, K., Kunieda, H., Takano, S., Tawara, Y., and Ohasi, T. 1991, *Astrophys. J.*, **366**, 88.

Bahcall, N. A., and Soneira, R. M. 1984, *Astrophys. J.*, **277**, 27.

Condon, J. J. 1974, *Astrophys. J.*, **188**, 279.

Day, C. S. R., Fabian, A. C., Edge, A. C., and Somak Raychaudhury 1991, *Monthly Notices Roy. Atron. Soc.*, **252**, 394.

Forman, W., Jones, C., Cominski, L., Julien, P., Murray, S., Peters, G., Tananbaum, H., and Giacconi, R. 1978, *Astrophys. J. Suppl.*, **38**, 357.

Gregory, S. A., and Thompson, L. A. 1978, *Astrophys. J.*, **222**, 784.

Hayashida, K., Inoue, H., Koyama, K., Awaki, H., Takano, S., Tawara, Y., Williams, O. R., Denby, M., Stewart, G. C., Turner, M. J. L., Makishima, K., and Ohashi, T. 1989, *Publ. Astron. Soc. Japan*, **41**, 373.

Hayashida, K. 1990, Ph. D. Thesis, The Univ. of Tokyo.

Jahoda, K., and Mushotzky, R. F. 1989, *Astrophys. J.*, **346**, 638.

Kellogg, E. M. 1978, *Astrophys. J. Letters*, **220**, L63.

Kondo, H. 1991, Ph. D. Thesis, The Univ. of Tokyo.

Makino, F., and ASTRO-C team 1987, *Astrophys. Letters Commun.*, **25**, 223.

Marshall, F. E., Boldt, E. A., Holt, S. S., Miller, R. B., Mushotzky, R. F., Rose, L. A., Rothschild, R. E., and Serlemitsos, P. J. 1980, *Astrophys. J.*, **235**, 4.

Murray, S. S., Forman, W., Jones, C., and Giacconi, R. 1978, *Astrophys. J. Letters*, **219**, L89.

Persic, M., Rephaeli, Y., and Boldt, E. 1988, *Astrophys. J. Letters*, **327**, L1.

Persic, M., Jahoda, K., Rephaeli, Y., Boldt, E., Marshall, F. E., Mushotzky, R. F., and Rawley, G. 1990, *Astrophys. J.*, **364**, 1.

Piccinotti, G., Mushotzky, R. F., Boldt, E. A., Holt, S. S., Marshall, F. E., Serlemitsos, P. J., and Shafer, R. A. 1982, *Astrophys. J.*, **253**, 485.

Pravdo, S. H., Boldt, E. A., Marshall, F. E., McKee, J., Mushotzky, R. F., Smith, B. W., and Reichert, G. 1979, *Astrophys. J.*, **234**, 1.

Turner, M. J. L., Thomas, H. D., Patchett, B. E., Reading, D. H., Makishima, K., Ohashi, T., Dotani, T., Hayashida, K., Inoue, H., Kondo, H., Koyama, K., Mitsuda, K., Ogawara, Y., Takano, S., Awaki, H. Tawara, Y., and Nakamura, N. 1989, *Publ. Astron. Soc. Japan*, **41**, 345.